

A New Fully Integrated High Frequency Full-Wave Rectifier Realization

Muhammed Emin Başak¹, Fırat Kaçar²

¹*Yildiz Technical University, Faculty of Naval Architecture and Maritime, Istanbul, Turkey*

²*Istanbul University, Dept. of Electrical and Electronics, Istanbul, Turkey*

Abstract: In this paper, a new fully integrated high frequency precise full-wave rectifier which consists of a floating current source (FCS) and four complementary MOS transistors is presented. The presented circuit has an appropriate zero crossing performance, linearity, low component count, and can be adapted to modern IC technologies. It is also suitable for monolithic integrated implementation. Rectifier performance is simulated based on 0.18 μ m CMOS technology. The proposed full-wave rectifier circuit provides an operating frequency more than 1 GHz, produces an input operating range from -300 mV to 300 mV and its power consumption is 825 μ W. LTSPICE simulation results of the circuit are presented which verify the workability of the proposed circuit. Noise analysis is also performed. The equivalent output noise of voltage mode rectifier at the 100 MHz is found as 7.13 nV/Hz. It also exhibits good temperature stability. The presented circuit does not require any passive component; therefore it is suitable for integrated circuit implementation. The proposed circuit exhibits the high frequency operation, the lower power consumption and has the simplest structure compared to all other available works.

Keywords: CMOS; full-wave rectifier; high frequency; floating current source; precision rectifier

Nov polno integriran visokofrekvenčni polnovalni usmernik

Izveček: V članku je predstavljen nov polno integriran natančen polnovalen usmernik, ki je sestavljen iz plavajočega tokovnega vira in štirih komplementarnih tranzistorjev MOS. Predstavljeno vezje ima primerne lastnosti ničnega prehoda, linearnosti, nizkega števila elementov in se g alahko uporabi v vseh modernih IC tehnologijah. Uporaben je tudi v monolitno integriranih vezjih. Lastnosti usmernika so simulirane v 0.18 μ m tehnologiji CMOS. Frekvenca predlaganega usmernika je več kot 1 GHz, vhodno območje od -300 mV do +300 mV, poraba 825 μ W. Opravljena je bila tudi analiza šuma. Usmernik ima dobro temperaturno stabilnost. Ker ne vsebuje pasivnih elementov je uporaben za integrirana vezja.

Ključne besede: CMOS; polnovalen usmernik; visoka frekvenca; plavajoči tokovni vir; natančen usmernik

*Corresponding Author's e-mail: fkacar@istanbul.edu.tr,

1 Introduction

Rectification is essential and demanding aspect of signal processing in instrumentation, measurement and control. Rectifiers have a variety of applications such as: signal processing, signal – polarity detectors, amplitude modulated signal detectors, AC voltmeters and ammeters, watt meters, RF demodulators, function fitting error measurements, RMS to DC conversions, sample and hold circuits, peak value detectors, clipper circuits.

Generally rectifier circuits are employed by using diodes, nevertheless, diodes cannot rectify the incoming signals whose amplitudes are less than their threshold voltages. For this reason, voltage-mode rectifiers containing active element based on operational amplifiers (op-amps),

diodes and resistors, have to be used. However, in consequence of the finite slew-rate and significant distortion during the zero crossing of the input signal effects caused by diode commutation, these circuits operate well only at low frequencies [1 - 5]. This is a small signal transient problem which cannot be solved by high slew-rate op-amps [6]. This problem has been overcome by the use of current mode technique [7-18] thanks to their higher operating frequency, wider bandwidth, larger dynamic range, and lower offset value at the zero crossing area compared with their voltage mode counterparts. However, some proposed rectifier circuits which were improved by the use of current conveyors (CCs) need either grounded or ungrounded resistors or some of them suffer from the limitation of high frequency. The present-

ed circuit in [7] uses a current differencing transconductance amplifier (CDTA) and two diodes at the operating frequency of 5 MHz. CDTA-based precision full-wave rectifier described in [8] exhibits a good performance at a frequency of 5MHz. The suggested circuits operating at a frequency up to 100 kHz utilize one current conveyor, one voltage conveyor, two diodes and grounded resistors [9-10]. The proposed circuit in [11] employs two differential difference current conveyors (DDCC), but it operates a few MHz. The circuit presented in [12], common-mode two-cell winner-takes-all (WTA) circuits, consisting of 21 transistors and two current sources, can be rectified at signals of frequency over 70MHz. A single second generation current conveyor (CCCII-) based precision full-wave rectifier circuit is reported in [13]. It employs (CCCII-) with three outputs, two CMOS transistor, and an ungrounded resistor, and has an operating frequency of 100 kHz. The circuit presented in [14] employs three current controlled conveyors and five resistors having a testing frequency of 100 kHz. The reported circuit in [15] utilizes two current conveyors and three NMOS transistors and its operating frequency is up to 100 MHz. The proposed circuit in [16] employing a dual-X current conveyor and three NMOS transistors, has been successfully tested by applying a sinusoidal input voltage with a frequency of 250 kHz. The reported rectifiers in [17-19] have been realized by all CMOS transistors, but they are half wave rectifiers. The proposed circuit in [20] operat-

ing at a few MHz is based on current conveyor and current mirror.

The realization of full-wave rectifier based on an operational transconductance amplifier (OTA) circuits is proposed in [21-27]. However a large number of active and passive components are used in these rectifiers and they have not shown good performance at higher frequencies. In [24], OTAs utilized as the full-wave rectifier are the only active elements, whereas they have been tested at lower frequencies. A three output operational transconductance amplifier with two complementary MOS transistors and a grounded resistor is used to realize non-inverting and inverting full-wave precision rectifiers in [25]. It rectifies high frequencies up to 200 MHz. The circuit presented in [26] is more suitable for IC implementation than previously OTA based circuits and confirms the operation frequency up to 200 MHz. This circuit consists of a dual-output OTA, junction diodes, and a MOS resistor. Another rectifier circuit uses OTA, four CMOS diodes, and a MOS resistor in its realization, providing operating frequency up to 300 MHz as well as good temperature stability in [27]. Table 1 presents the comparison of the proposed precision full-wave rectifier with other designs. The employed full-wave rectifier is superior to the previously proposed full-wave rectifiers in terms of the power consumption, the number of components, and the operating frequency as seen in Table 1.

Table 1: Comparison of the various rectifiers in literature

Article	DC Supply Voltage	Technology	Power Compsumption	Operating Frequency	Components	Year
Proposed	± 2.4V	0.18 μm	825 μW	1 GHz	8 × MOSFET + 2 × current sources	-
[3]	± 1V	-	-	100 kHz	OPA1 + OPA2 + 2 × diodes + 3 × Resistors	2007
[4]	± 1V	-	-	1 MHz	AD817 × 2 + AD633 × 3 + AD711 + R	2010
[5]	± 1V	-	-	1 MHz	AD817 × 2 + AD633 × 3 + AD711 + Resistor	2011
[7]	± 1V	-	-	5 MHz	CDTA + 2 × Schottky Diodes	2010
[9]	-	-	-	500 kHz	Current Conveyor + Voltage Conveyor	2010
[10]	± 1V	-	-	1 MHz	2×CCII + 2 diodes or CCII + VC+2 diodes	2011
[11]	± 2.5V	0.5 μm	-	1 MHz	2×DDCCI	2011
[13]	± 2.5V	-	-	5 kHz	CCCII + 2×CMOS + R	2007
[15]	±1.25V	0.25 μm	-	10 MHz	23 MOSFET	2006
[16]	±1.25V	0.25 μm	-	1 MHz	DXCCII (20 CMOS) + 3×NMOS	2008
[19]	-	-	-	200 MHz	26 CMOS + 1 current supply	2006
[20]	± 1.5V	0.5 μm	-	10 MHz	33 MOSFET	2007
[23]	± 5V	-	-	10 kHz	4×OTA or 5×OTA	2007
[24]	± 5V	0.5 μm	-	200 MHz	OTA (24MOSFET) + 2 MOS + Resistor	2009
[25]	± 5V	0.5 μm	7.9 mW	300 MHz	24 MOSFET	2010
[27]	± 1.2V	0.5 μm	-	250 MHz	31 MOSFET	2006

Floating current source (FCS) was firstly introduced to be used as an output stage for current-mode feedback amplifiers by Arbel and Goldminz in 1992 [28]. Following that, the FCS was used as the output stage of the accurate CCII- proposed in [29-30] to perform the required current conveying action. The FCS has also been used in the realization of fully differential voltage second generation current conveyor [31]. Then, [32] presented two novel floating current source based CMOS negative second generation current conveyor (CCII-).

In this paper, a new circuit for realizing full wave rectifier employing a floating current source, two CMOS diodes, and a MOS resistor, is proposed. The proposed circuit was simulated by LTSPICE simulator with 0.18 μm CMOS model obtained through TSMC (Taiwan Semiconductor Manufacturing Company, Limited). The advantages of the presented structure over the previously presented rectifiers are as follows:

- The presented structure is very compact and consists of an FCS and four CMOS transistors, thus enjoying a simpler structure compared to all other available works [1-27].
- The proposed circuit, verified the operation frequency up to 1 GHz, which is the highest frequency when compared with the previously published rectifiers.
- It does not require any passive component; therefore it is suitable for integrated circuit (IC) implementation.
- It provides high precision voltage rectifying.
- This rectifier has the lowest power consumption (825 μW) in comparison with the hitherto published rectifiers [1-27].

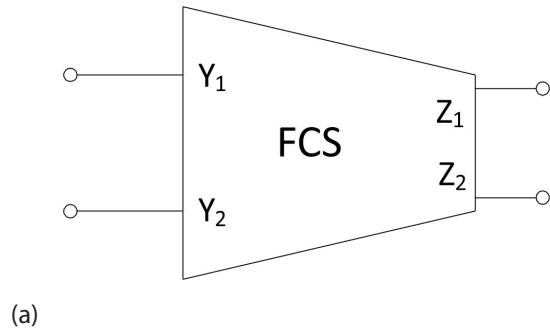
2 The Floating Current Source

Floating current source circuit can be viewed as two differential pairs connected in parallel; an NMOS pair and a PMOS pair. It is assumed that $M_1 - M_2$ and $M_3 - M_4$ are matched and operate in the saturation region for the NMOS pair and PMOS pair, respectively. Symbol of the FCS and its MOSFET implementation is shown in Fig. 1 (a) and Fig. 1 (b), respectively. [28] provides two balanced output currents satisfying Kirchhoff's current law. The equations of the output currents are given in below.

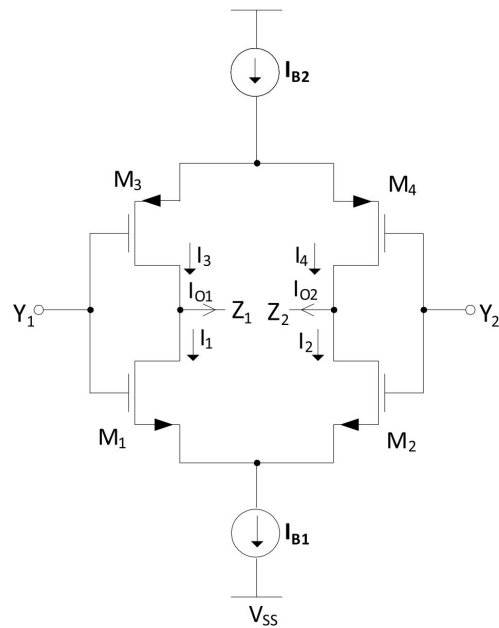
$$I_{B2} = I_{B1} + I_{O1} + I_{O2} \tag{1}$$

$$I_{B2} = I_{B1} \tag{2}$$

$$I_{O1} = -I_{O2} \tag{3}$$



(a)



(b)

Figure 1: (a) Symbol of floating current source circuit (b) MOSFET implementation of floating current source circuit [28]

It is assumed that $M_1 - M_2$ and $M_3 - M_4$ are equal transistors and so we can say that the transconductance of M_1 is equal of transconductance of M_2 ($g_{m1} = g_{m2}$) and transconductance of M_3 is equal of transconductance of M_4 ($g_{m3} = g_{m4}$). Then the transconductances of the FCS circuit (g_{mo1} and g_{mo2}) are given in Equation (4). The output impedances of the FCS structure are given in Equation (5).

$$g_{mo1} = -g_{mo2} = \frac{(g_{m1} + g_{m3})}{2} \tag{4}$$

$$R_{o1} = R_{o2} = \left[\left(\frac{g_{m3}g_{ds3}}{g_{m3} + g_{m4}} \right) + \left(\frac{g_{m1}g_{ds1}}{g_{m1} + g_{m2}} \right) \right]^{-1} = \frac{2}{g_{ds1} + g_{ds3}} \tag{5}$$

Two balanced output currents are given by [33];

$$I_{o1} = -I_{o2} = -\frac{1}{2}V_d \left[\sqrt{k_n} \sqrt{I_{B1} - \frac{k_n V_d^2}{4}} \right] + \sqrt{k_p} \sqrt{I_{B1} - \frac{k_p V_d^2}{4}} \quad (6)$$

where $V_d = V_1 - V_2$

V_1 and V_2 are the voltages applied to Y_1 and Y_2 , respectively.

k_n is the NMOS transconductance parameters given by

$$k_n = \mu_n C_{OX} \frac{W_1}{L_1} \quad (7)$$

k_p is the PMOS transconductance parameters given by

$$k_p = \mu_p C_{OX} \frac{W_3}{L_3} \quad (8)$$

where

μ =mobility of carrier;

C_{ox} =gate capacitance per unit area;

W, L = channel width and channel length of the MOS transistor, respectively;

I_{B1}, I_{B2} = bias currents;

3 Proposed Full-Wave Rectifier Circuit

The basis of proposed full-wave rectifier is shown in Fig. 2. It is composed of three parts which are FCS, four diodes and resistor. A FCS is used to convert the voltage into two currents through the terminals p and n, then the four diodes rectify these currents. Afterwards, resistor converts the rectified current into the output voltage. The voltage source V_b is approximately equal to the sum of the threshold voltage of D_1 and D_2 and keep them ready for conduction [6].

Cross-section of NMOS and PMOS transistors in a p-substrate CMOS process are presented in Fig. 3. The structure of M_{D1} and M_{D2} are used to replace diodes D_1 to D_4 [26]. The diodes D_1 and D_2 are the junction diodes established between p-substrate and n+ diffusion of the drain and source regions and D_3 and D_4 are the junction diodes established between n-well and p+ diffusion of the drain and source regions. These diodes operate as a precision rectifier.

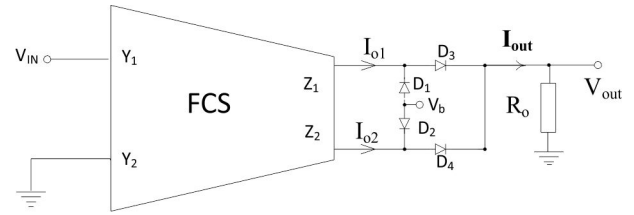


Figure 2: The principle of the proposed rectifier

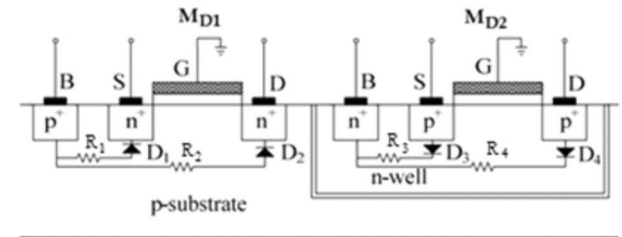


Figure 3: Cross-section of M_{D1} and M_{D2} transistors in a p-substrate CMOS process [26].

The proposed high precision full-wave rectifier in detail is shown in Fig. 4. The FCS is consisted of four MOS transistors (M_1 - M_4) and two bias currents I_{B1} and I_{B2} . M_{D1} and M_{D2} are used as four diodes as described the above and M_{R1} and M_{R2} are operated as a MOS resistor in the saturation region. The resistance value of MOS resistor R_o can be expressed as;

$$R_o = \frac{1}{2\mu_0 C_{OX} (W/L) (V_{GS} - V_{TH})} \quad (9)$$

where, V_{TH} is the threshold voltage and $V_{GS} = V_{DD} = |V_{SS}|$.

The relativity of the positive and negative polarity input voltage and output voltage can be expressed in below from the definition;

$$V_{in} < 0; I_{out} = -\frac{g_{m1} + g_{m3}}{2} V_{in}, V_{out} = I_{out} \cdot R_o \quad (10)$$

$$V_{in} > 0; I_{out} = \frac{g_{m1} + g_{m3}}{2} V_{in}, V_{out} = I_{out} \cdot R_o \quad (11)$$

The proposed full-wave rectifier is simulated using the schematic implementation shown in Fig. 4. The voltage sources V_{DD1} and V_{SS1} are ± 2.4 V and V_{DD2} and V_{SS2} are ± 0.75 V. The TSMC 0.18 μ m CMOS model parameters, which are shown in Table 2, are used in the simulations. The W/L parameters of MOS transistors are 1.98 μ m/0.18 μ m for M_1, M_2 ; 1.36 μ m/1.36 μ m for M_3, M_4 ; 0.36 μ m/0.36 μ m for M_{D1}, M_{D2} ; and 1.36 μ m/0.72 μ m for M_{R1}, M_{R2} . Bias currents are 165 μ A for both I_{B1} and I_{B2} and bias voltage V_b is 0.7 V.

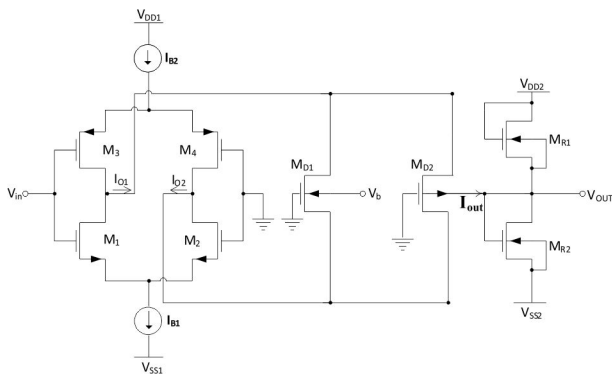


Figure 4: Proposed full-wave rectifier circuit.

4 Simulation Results

The DC transfer characteristic of the proposed full-wave rectifier is shown in Fig. 5, which shows the operating voltage ranging from -300mV to 300mV of the input voltage. Diodes and Op-amp based conventional rectifiers are resulting in significant distortion during the zero crossing of the input signal. The zero crossing region of the DC transfer characteristic is shown in Fig. 6. In this figure, the offset is found as $54.8\ \mu\text{V}$ which is the lowest value when compared to all other available works [1-27].

The input (V_{in}) and output signals of inverting full-wave precision rectifier at 100 MHz and 1 GHz frequencies are shown in Fig. 7. The period of the rectified signal (T), as seen as the stabilized region in this figure, is equal to 5 ns and 0.5 ns when the input signal's frequency is 100 MHz and 1 GHz, respectively. It can also be clearly observed from the figure that the behavior of the floating current source based full-wave rectifier is very satisfactory. Hence, the proposed rectifier can be used to process the signals at the frequencies up to 1 GHz without causing any major distortions. Applying the $300\ \text{mV}_{\text{peak}}$ sine wave at the input of the proposed fullwave rectifier, the input and output signals at a frequency of 100 MHz is shown in Fig. 8. The power consumption of proposed rectifier is $825\ \mu\text{W}$ which is the lowest value when compared to all other available works [1-27].

We simulate the temperature performance of the DC transfer characteristics of the proposed full-wave rectifier for the varied temperature ranging from 0°C to 100°C as shown in Fig. 9. The zero crossing regions of the DC transfer characteristic's among different temperatures are shown in Fig. 10. This figure shows that there is only a small amount of difference of the offsets among different temperatures. The offsets for different temperatures are obtained from the LTSPICE simulation results as shown in Fig. 10, given in Table 3.

Table 2: 0.18 μm TSMC model parameters used in the simulation

```
.MODEL NMOS (LEVEL = 7 VERSION = 3.1 TNOM = 27 TOX=4.1E-9 XJ = 1E-7 NCH = 2.3549E17 VTH0 = 0.3725327
K1 = 0.5933684 K2 = 2.050755E-3 K3 = 1E-3 K3B = 4.5116437 W0 = 1E-7 NLX = 1.870758E-7 DVT0W = 0 DVT1W = 0
DVT2W = 0 DVT0 = 1.3621338 DVT1 = 0.3845146 DVT2 = 0.0577255 U0 = 259.5304169 UA = -1.413292E-9 UB =
2.229959E-10 UC = 4.525942E-11 VSAT = 9.411671E4 A0 = 1.7572867 AGS = 0.3740333 B0 = -7.087476E-9 B1 = -1E-7
KETA = -4.331915E-3 A1 = 0 A2 = 1 RDSW = 111.886044 PRWG = 0.5 PRWB = -0.2 WR = 1 WINT = 0 LINT = 1.701524E-8 XL = 0
XW = -1E-8 DWG = -1.365589E-8 DWB = 1.045599E-8 VOFF = -0.0927546 NFACTOR = 2.4494296 CIT = 0 CDSC = 2.4E-4 CD-
SCD = 0 CDSCB = 0 ETA0 = 3.175457E-3 ETAB = 3.494694E-5 DSUB = 0.0175288 PCLM = 0.7273497 PDIBLC1 = 0.1886574
PDIBLC2 = 2.617136E-3 PDIBLCB = -0.1 DROUT = 0.7779462 PSCBE1 = 3.488238E10 PSCBE2 = 6.841553E-10
PVAG = 0.0162206 DELTA = 0.01 RSH = 6.5 MOBMOD = 1 PRT = 0 UTE = -1.5 KT1 = -0.11 KT1L = 0 KT2 = 0.022 UA1 = 4.31E-9
UB1 = -7.61E-18 UC1 = -5.6E-11 AT = 3.3E4 WL = 0 WLN = 1 WW = 0 WWN = 1 WWL = 0 LL = 0 LLN = 1 LW = 0 LWN = 1 LWL = 0
CAPMOD = 2 XPART = 0.5 CGDO = 8.53E-10 CGSO = 8.53E-10 CGBO = 1E-12 CJ = 9.513993E-4 PB = 0.8 MJ = 0.3773625
CJSW = 2.600853E-10 PBSW = 0.8157101 MJSW = 0.1004233 CJSWG = 3.3E-10 PBSWG = 0.8157101 MJSWG = 0.1004233
CF = 0 PVTH0 = -8.863347E-4 PRDSW = -3.6877287 PK2 = 3.730349E-4 WKETA = 6.284186E-3 LKETA = -0.0106193
PU0 = 16.6114107 PUA = 6.572846E-11 PUB = 0 PVSAT = 1.112243E3 PETA0 = 1.002968E-4 PKETA = -2.906037E-3 )
.MODEL PMOS ( LEVEL = 7 VERSION = 3.1 TNOM = 27 TOX = 4.1E-9 XJ = 1E-7 NCH = 4.1589E17 VTH0 = -0.3948389
K1 = 0.576352 K2 = 0.0289236 K3 = 0 K3B = 13.8420955 W0 = 1E-6 NLX = 1.337719E-7 DVT0W = 0 DVT1W = 0 DVT2W
= 0 DVT0 = 0.5281977 DVT1 = 0.2185978 DVT2 = 0.1 U0 = 109.9762536 UA = 1.325075E-9 UB = 1.577494E-21 UC =
-1E-10 VSAT = 1.910164E5 A0 = 1.7233027 AGS = 0.3631032 B0 = 2.336565E-7 B1 = 5.517259E-7 KETA = 0.0217218 A1
= 0.3935816 A2 = 0.401311 RDSW = 252.7123939 PRWG = 0.5 PRWB = -0.0158894 WR = 1 WINT = 0 LINT = 2.718137E-
8 XL = 0 XW = -1E-8 WG = -4.363993E-8 DWB = 8.876273E-10 VOFF = -0.0942201 NFACTOR = 2 CIT = 0 CDSC =
2.4E-4 CDSCD = 0 CDSCB = 0 ETA0 = 0.2091053 ETAB = -0.1097233 DSUB = 1.2513945 PCLM = 2.1999615 PDIBLC1 =
1.238047E-3 PDIBLC2 = 0.0402861 PDIBLCB = -1E-3 DROUT = 0 PSCBE1 = 1.034924E10 PSCBE2 = 2.991339E-9 PVAG
= 15 DELTA = 0.01 RSH = 7.5 MOBMOD = 1 PRT = 0 UTE = -1.5 KT1 = -0.11 KT1L = 0 KT2 = 0.022 UA1 = 4.31E-9 UB1 =
-7.61E-18 UC1 = -5.6E-11 AT = 3.3E4 WL = 0 WLN = 1 WW = 0 WWN = 1 WWL = 0 LL = 0 LLN = 1 LW = 0 LWN = 1 LWL
= 0 CAPMOD = 2 XPART = 0.5 CGDO = 6.28E-10 CGSO = 6.28E-10 CGBO = 1E-12 CJ = 1.160855E-3 PB = 0.8484374
MJ = 0.4079216 CJSW = 2.306564E-10 PBSW = 0.842712 MJSW = 0.3673317 CJSWG = 4.22E-10 PBSWG = 0.842712
MJSWG = 0.3673317 CF = 0 PVTH0 = 2.619929E-3 PRDSW = 1.0634509 PK2 = 1.940657E-3 WKETA = 0.0355444 LKETA
= -3.037019E-3 PU0 = -1.0227548 PUA = -4.36707E-11 PUB = 1E-21 PVSAT = -50 PETA0 = 1E-4 PKETA = -5.167295E-3 )
```

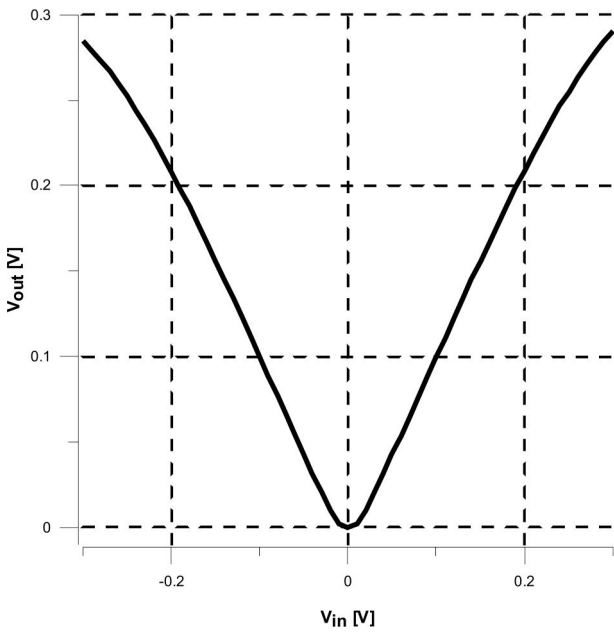


Figure 5: DC transfer characteristic of the proposed rectifier.

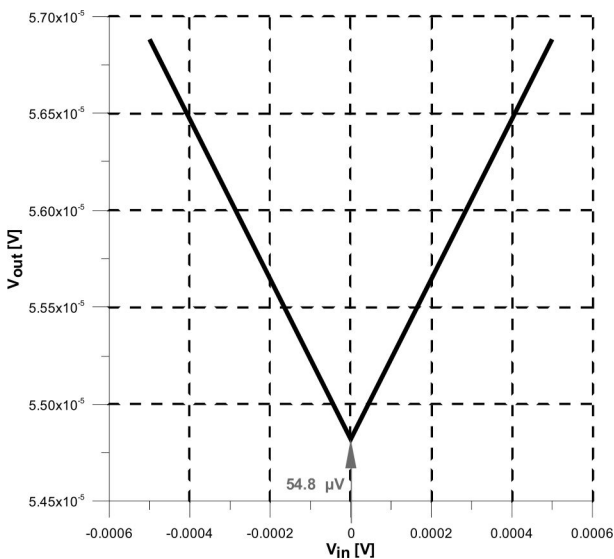


Figure 6: Simulated results for DC characteristic at zero crossing regions.

The time domain response of the proposed full-wave rectifier of a 100 MHz frequency at different temperatures is shown in Fig. 11 and its details are shown in Fig.12. The offset values of the time domain response at the zero crossing regions are given in Table 3 for various temperatures. The peak outputs V_{out} values are also given in Table 3 for various temperatures. This table shows that difference is negligible between the output voltages at zero crossing regions and peak outputs V_{out} values for different temperatures. Therefore, we concluded that the proposed full-wave rectifier provides good temperature stability without compensation cir-

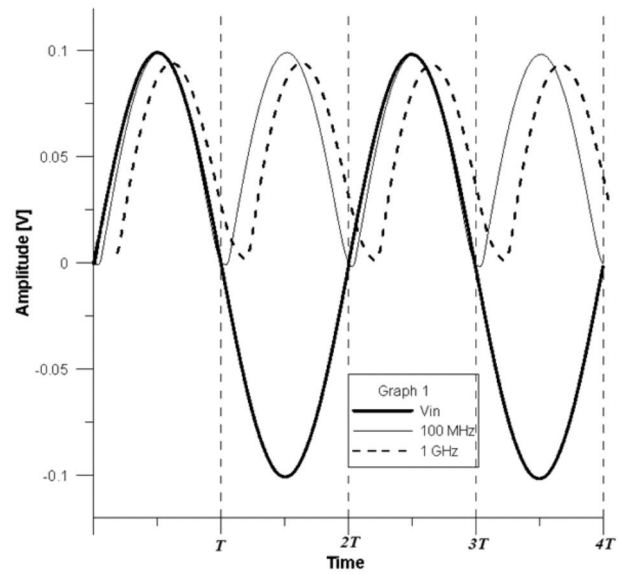


Figure 7: Input (sinusoidal) and rectified output waveforms of inverting full-wave precision rectifier of Fig. 4 at 100 MHz and 1 GHz frequencies.

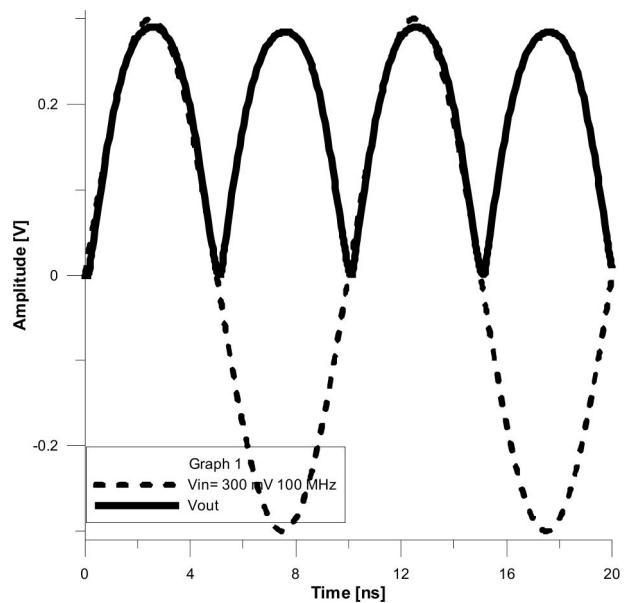


Figure 8: Applying the 300 mV sine wave at the input, input and rectified output waveforms of inverting full-wave precision rectifier at a frequency of 100 MHz.

cuit. Output noise behaviors of the proposed rectifiers with respect to frequency have also been simulated. The equivalent output noise of voltage mode rectifier at 100 MHz frequency is found as $7.13 \text{ nV}/\sqrt{\text{Hz}}$.

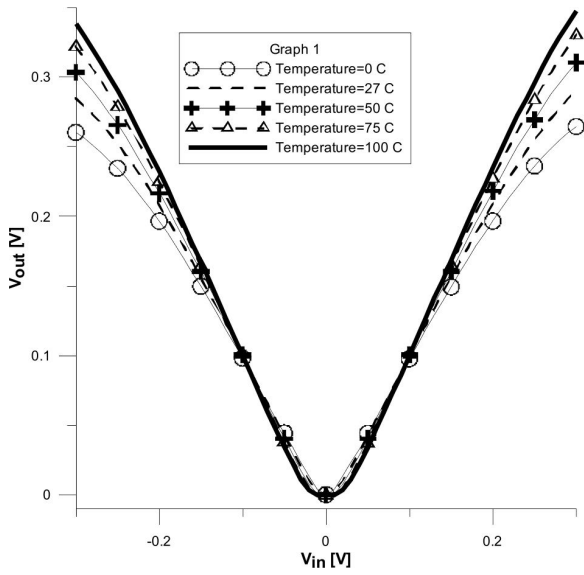


Figure 9: DC transfer characteristic of the proposed full-wave rectifier of a 100MHz frequency for different temperatures.

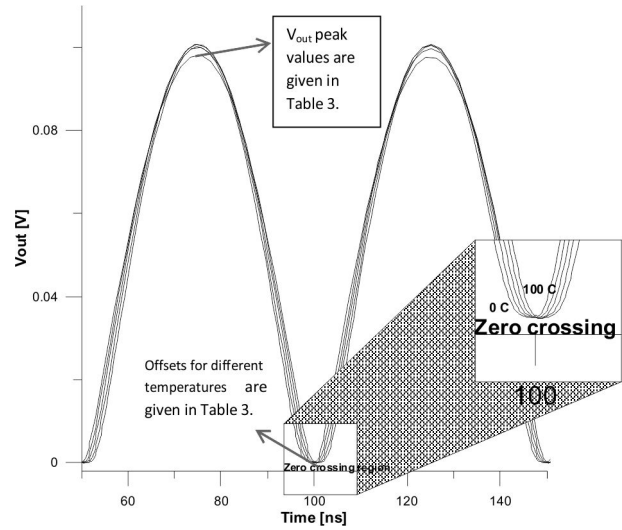


Figure 11: Time domain response of the proposed full-wave rectifier of a 100 MHz frequency at different temperatures.

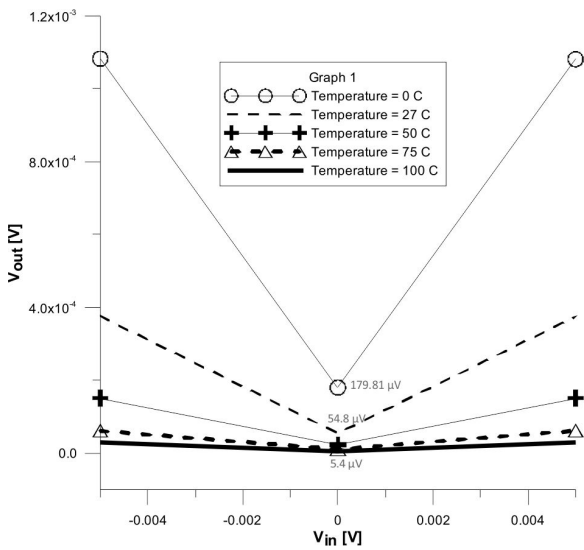


Figure 10: Simulated results for DC characteristics at zero crossing regions among different temperatures.

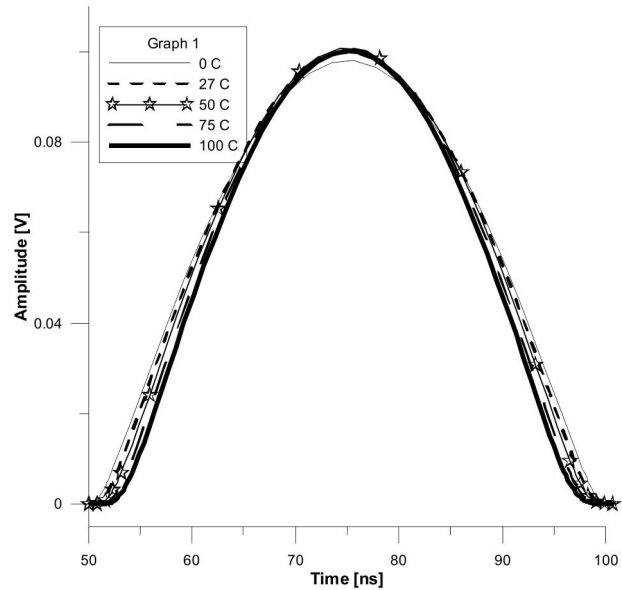


Figure 12: The detailed time domain response of the proposed full-wave rectifier of a 100 MHz frequency at different temperatures.

Table 3: The performance of the output waveform of the proposed rectifier at different temperatures.

Temperature	Offsets (DC characteristics)	Offsets (time domain)	Vout peak (time domain)
0°C	179.81 μV	304.11 μV	97.486 mV
27°C	54.8 μV	41.33 μV	99.611 mV
50°C	23.5 μV	-67.03 μV	100.409 mV
75°C	10.7 μV	-205.17 μV	100.496 mV
100°C	5.4 μV	-302.78 μV	100.232 mV

5 Conclusion

In this paper, a new fully integrated high frequency full-wave rectifier which has been used the least CMOS transistor, has been proposed. Its operating frequency is up to 1 GHz. It does not involve any passive component; thus it is appropriate for integrated circuit implementation. It provides high precision voltage rectifying. The proposed full-wave rectifier provides excellent temperature stability without compensation circuit. LT-SPIICE simulations confirm the operability of this circuit in a wide frequency range. The fascinating character-

istics of the proposed rectifier are the high frequency operation (up to 1 GHz), the lowest component count (10 components), the lowest power consumption (825 μ W), the lowest offset value (54.8 μ V) and suitable for IC fabrication.

6 References

1. Gift S. J. G., An improved precision full-wave rectifier, *International Journal of Electronics*, vol. 89, pp. 259-265, 2002.
2. Gift S. J. G., New precision rectifier circuits with high accuracy and wide bandwidth, *International Journal of Electronics*, vol. 92, pp. 601-617, 2005.
3. Gift S. J. G., Versatile precision full-wave rectifiers for instrumentation and measurements, *IEEE Transactions on Instrumentation and Measurements*, vol. 56, pp. 1703-1709, 2007.
4. Sahu, P. P., Singh, M., Baishya, A., A novel versatile precision full-wave rectifier, *IEEE Transactions on Instrumentation and Measurements*, vol. 59, pp. 2742-2746, 2010.
5. Sahu, P. P., Singh, M., Baishya, A., New low-voltage full wave rectification technique without a diode, *IET Circuits, Devices and Systems*, vol. 5, pp. 33-36, 2011.
6. Toumazou, C., Lidgey F. J. and Chattong S., High frequency current conveyor precision full-wave rectifier, *Electronics Letters*, vol. 30, No.10, pp. 745-746, 1994.
7. Khateb, F., Vavra, J., Biolek, D., A novel current-mode full-wave rectifier based on one CDTA and two diodes, *Radioengineering*, vol. 19, pp. 437-445, 2010.
8. Biolek, D., Hancioglu, E., Keskin, A. U., High-performance current differencing transconductance amplifier and its application in precision current-mode rectification, *International Journal of Electronics and Communications*, vol. 62, pp. 92-96, 2008.
9. Koton, J., Herencsar, N., Vrba, K. Minimal configuration precision full-wave rectifier using current and voltage conveyors, *IEICE Electronics Express*, vol. 7, pp. 844-849, 2010.
10. Koton, J., Herencsar, N., Vrba, K., Current and voltage conveyors in current and voltage-mode precision full-wave rectifiers, *Radioengineering*, vol. 20, pp. 19-24, 2011.
11. Kumngern, M. Precision full-wave rectifier using only two DDCCs. *Circuits and Systems*, vol. 2, no. 3, pp. 127-132, 2011.
12. Koton, J., Lahiri, A., Herencsar, N., Vrba, K. Current-mode dual-phase precision full-wave rectifier using current-mode two-cell winner-takes-all (WTA) circuit. *Radioengineering*, 2011, vol. 20, pp. 428-432.
13. Maheshwari, S., Current controlled precision rectifier circuits, *Journal of Circuit Systems, and Signal Components*, vol. 16, pp. 129-138, 2007.
14. Anuntahirunrat K., Tangsrirat W., Riewruja V. and Surakamponorn W., Sinusoidal frequency doubler and full-wave rectifier based on translinear current-controlled current conveyors, *International Journal of Electronics*, 91, pp. 227-239, 2004.
15. Yuce, E., Minaei, S., Cicekoglu, O., Full-wave rectifier realization using only two CCII+s and NMOS transistors, *International Journal of Electronics*, vol. 93, pp. 533-541, 2006.
16. Minaei, S., Yuce, E., A new full-wave rectifier circuit employing single dual-X current conveyors, *International Journal of Electronics*, vol. 95, pp. 777-784, 2008.
17. Chaoui, H., CMOS high-frequency rectifier with unity voltage gain, *Electronics Letters*, vol. 31, pp. 717-718, 1995.
18. Monpapassorn, A., Dejhan, K., Cheevasuvit, F. CMOS dual output current mode half-wave rectifier, *International Journal of Electronics*, vol. 88, pp. 1073-1084, 2001.
19. Kumngern, K., Knobnob, B., Dejhan, K., High frequency and high precision CMOS half-wave rectifier, *Circuits, Systems and Signal Processing*, vol. 29, pp. 815-836, 2010.
20. Kumngern, M., Dejhan, K., Current conveyor-based versatile precision rectifier, *WSEAS Transactions on Circuits and Systems*, vol. 7, pp. 1070-1079, 2008.
21. Sanchez-Sineccio, E., Ramirez-Angulo, J., Linares-Barranco, B., Rodriguez-Vazquez, A. Operational transconductance amplifier-based nonlinear function syntheses, *IEEE Journal of Solid-State Circuits*, vol. 24, pp. 1576-1586, 1989.
22. Heim, P., Krummenacher, F., Vittoz, E. CMOS full-wave operational transconductance rectifier with improved DC transfer characteristic, *Electronics Letters*, vol. 28, pp. 333-334, 1992.
23. Ramirez-Angulo, J., High frequency, low voltage CMOS diode, *Electronics Letters*, vol. 28, pp. 298-299, 1992.
24. Jongkunstidchai, C., Fongsamut, C. Kumwachara, K., Surakamponorn, W. Full-wave rectifiers based on operational transconductance amplifiers, *International Journal Electronics and Communications*, vol. 61, pp. 195-201, 2007.
25. Minhaj, N., OTA-based non-inverting and inverting precision full-wave rectifier circuits without diodes, *International Journal of Recent Trends in Engineering*, vol. 1, pp. 72-75, 2009.
26. Kumngern, M., High frequency and high precision CMOS full-wave rectifier, *In Proceedings of IEEE In-*

- ternational Conference on Communication Systems (ICCS 2010)*, Singapore, pp. 5–8, 2010.
27. Kumngern, M., Dejhan, K., High frequency and high precision CMOS full-wave rectifier, *International Journal of Electronics*, vol. 93, pp. 185-199, 2006.
 28. Arbel A. F., Goldminz L., Output Stage for Current-Mode Feedback Amplifiers, Theory and Applications, *Analog Integrated Circuits and Signal Processing*, pp. 234–255, 1992.
 29. Arbel A. F., Towards A Perfect CMOS CCII, *Analog Integrated Circuits and Signal Processing*, pp. 119–132, 1997.
 30. Awad I. A., Soliman A. M., New CMOS Realization of the CCII-, *IEEE Trans. Circuits, Systems*, pp. 460–463, 1999.
 31. Sobhy E. A., Soliman A. M., Realizations of Fully Differential Voltage Second Generation Current Conveyor with An Application, *International J. of Circuit Theory and Applications*, vol. 18, Issue 5, 441-452, 2010.
 32. Mostafah., and Soliman A. M., Novel Low-Power Accurate Wide-band CMOS Negative Second Generation Current Conveyor Realizations Based on Floating Current Source Building Blocks, *Science and Technology for Humanity (TIC-STH), 2009 IEEE Toronto International Conference*, pp. 720 – 725, 2009.
 33. Youssef M. A., Soliman A. M., A Modified CMOS Balanced Output Transconductor with Extended Linearity, *Analog Integrated Circuits and Signal Processing*, pp. 239–244, 2003.

Arrived: 14. 07. 2014

Accepted: 09. 02. 2015